EFFICIENCY OF SOUND ENERGY DECAY ANALYSIS IN AUDITORIA

N. Xiang Graduate Program in Architectural Acoustics, Rensselaer Polytechnic Institute, USA
Z. Sü Gül Department of Architecture, Bilkent University, Turkey

0 ABSTRACT

Recent auditorium acoustics practice has included coupled-volume systems in several performing arts venues. This has stimulated research activities on acoustics in the coupled-volume systems. Based on experimentally measured room impulse responses acquired from existing auditoria, and several historically significant worship spaces, this paper addresses the challenges of analysing single-slope and multiple-slope sound energy decays often encountered in the experimentally measured room impulse responses in these venues. The analysis engages a parametric model of Schroeder decay functions, that decomposes the Schroeder decay data into single or multiple exponential decays along with a noise term. The model has been well validated using many experimental data. Several advanced analysis methods based on the decay model, such as nonlinear regressions, Bayesian probabilistic inference, and artificial neural networks have emerged to cope with analysis challenges raised in auditorium acoustics practice. This paper discusses conditions of implementing Schroeder integration for a higher efficiency of the numerical analysis and clarifies some unreasonable expectations/interpretations of Schroeder decay data.

1 INTRODUCTION

Recent design practice has intentionally implemented coupled-volume systems in several performing arts venues, including music practice rooms.[1] The intention is supposed to achieve two desirable, yet competing attributes of auditory perception, reverberance and clarity. In a recent effort of analyzing historically significant worship spaces,[2] analysis of non-single exponential decays of sound energy has also been in need. In these applications, acousticians are challenged to determine energy decay characteristics from Schroeder decay functions,[3] that may be characterized by single- or multiple decay rates. Another challenge is a specific characteristics being inherent in Schroeder decay function that strongly deviates from exponential decays of single-rate or multiple-rate nature. These challenges have stimulated active research in auditorium acoustics. Several advanced analysis methods have emerged including nonlinear regressions,[4] Bayesian decay analysis[5] and artificial neural networks.[6]

2 STEADY-STATE ENERGY DECAYS

Nowadays steady-state sound energy decays are predominantly accomplished using Schroeder integral [3] of room impulse responses (RIRs) to obtain an energy decay function,

$$D(t_k) \propto \sum_{t=t_k}^{t_K} h^2(t) \qquad \text{for} \qquad 0 \le k \le K\ , \tag{1}$$

with K being the total number of discrete points of RIR $h(t)$, $t_0 = 0,$ and constant time quantity t_K is the *upper limit of integration* (ULI).

Xiang[4] established a parametric model, later extended it to a more generalized form [5] as

$$H(\mathbf{\Theta}, t_k) = \theta_0(t_k - t_K) + \sum_{s=1}^{S} \theta_{(2s-1)}\left[\mathrm{e}^{-\theta_{2s}t_k} - \mathrm{e}^{-\theta_{2s}t_K}\right], \tag{2}$$

in coping with challenges of analyzing potentially S *number of decay rates*, where $\mathbf{\Theta} = \{\theta_0, \theta_1, \dots, \theta_{2S}\}$, collectively contains $2S + 1$ decay parameters, with $\theta_{2s} = 13.8/T_s$. Then acousticians are dealing with S number of *decay times*/T_s and S number of initial coefficients $\theta_{(2s-1)}$. The first term on the right-hand side of Eq. (2) represents a linearly decaying function, it results from background noise inevitably

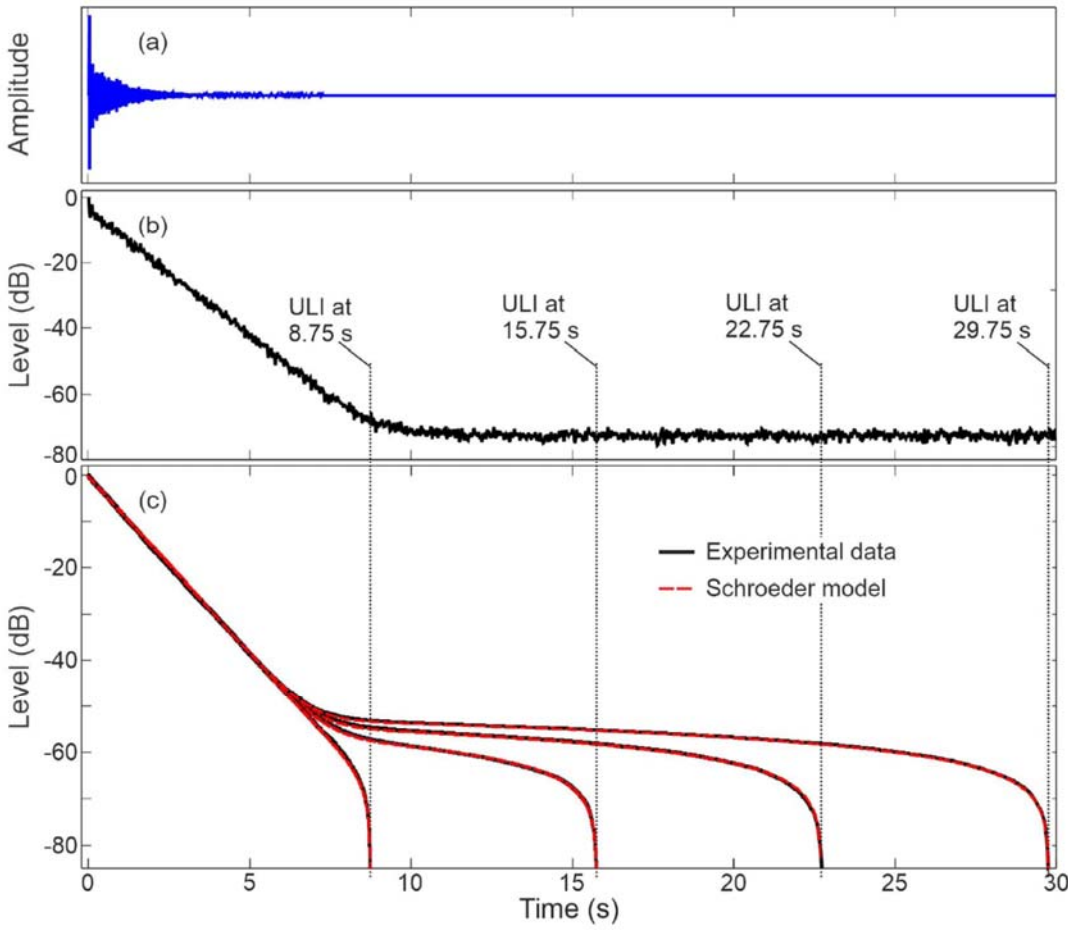

Figure 1. Comparison of Schroeder decay curves and decay models with the energy-time curve, the original room impulse response experimentally measured in a worship space.

contained in experimentally measured data, this term is called *noise term*.[5] Due to this term, the Schroeder decay curves when presenting them graphically, deviate drastically from the exponential decays.[4]

To highlight the characteristics of Schroeder decay functions derived using Eq. (1) and their respective models in Eq.(2), Figure 1 (a) illustrates one RIR, experimentally measured in a well-known worship space in Europe. Figure 1 (b) shows its corresponding energy RIR $h(t)$, graphically presented in levels [dB], often termed *energy-time curve* (ETC) in practice. Figure 1 (c) illustrates the corresponding Schroeder decay curves at different ULIs along with their prediction model curves. Irrespective of different ULIs, the parametric model curves well predict the experimentally measured Schroeder decay curves.

Characteristic curvatures towards the respective ULIs; the ends of the Schroeder decay curves, were often confused in the literature. These characteristic curvatures are predominantly described by the noise term on the right-hand side of Eq. (2). It is a typical logarithmic behavior of the linearly decaying function $\theta_0(t_k - t_K)$ for $t_k \rightarrow t_K$, no matter how big the ULI value is. The noise term $\theta_0(t_k - t_K)$ also captures different background noise levels of experimentally measured RIRs. Figure 2 showcases three Schroeder decay curves measured in the same source-receiver location in a scale model, yet different noise levels (PNR = 50, 54, 58 dB). The predicted curves indicate that the model in Eq. (2) also accurately captures changes in different noise levels, in which the three

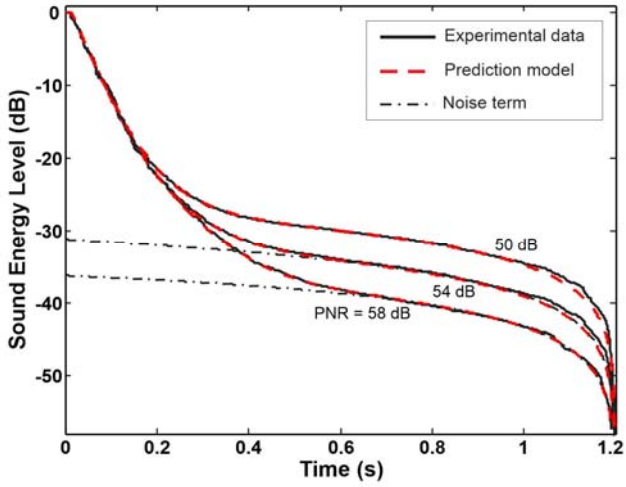

Figure 2. Comparison of Schroeder decay curves experimentally measured from the same location, yet at different peak-to-noise ratio. Two lowest noise terms are also plotted.

modeled curves are predicted by the same decay parameters $\theta_1, \ldots \theta_4$, but only with three different values of θ_0. Note that these Schroeder curves in this specific example are of double-slope nature. It is unhelpful to fit a linear slope to the curvature immediately before the ULIs as shown in Fig. 1 (c) and in Fig. 2. These figures clarify such an unreasonable expectation of Schroeder decay curves (being exponential decays only).

Another unreasonable expectation is because the Schroeder decay curves, graphically presented in logarithmic scale (in level dB), would erroneously be fitted by straight lines. When involving the correct models, the model-based analysis, such as that in Eq. (2) demonstrates well agreed model curves with the experimental curves, clarifies such an unreasonable expectation which is simply based on wrong models. The state-of-the-art decay analysis is better suited using the correct models [Eq.(2)].

The third vague interpretation lies in the effort to truncate the RIR suitably, for example, as the curves labeled by ULI at 8.73 s in Fig. 1 (c) or estimate that characteristic curvature in replacing it by a linearly decaying extension. Such efforts will possibly destroy the inherent decay characteristics when the decay process features non-single exponential decays, rather multiple ones. This is challenging, because the experimenter would not know beforehand how many decay slopes there are in the data.

Since the well validated model supports acousticians with fully understanding of Schroeder decay functions, the above-mentioned efforts in the past due to unreasonable expectations/interpretations become redundant. Thus, they should be avoided in the future. Rather, the model-based analysis using the correct models in Eq. (2) yields rigorous solutions.

3. RESOLUTION OF DECAY FUNCTIONS

When presenting Schroeder integration as indicated by discrete time variable t_k, it is not necessarily useful to integrate RIRs experimentally measured at original sampling rate (integration step), for instance at f_s = 44.1/48 kHz. Instead, it is sufficient to integrate the energy impulse responses at much lower temporal resolution by stepping t_k in rather larger intervals for most of room-acoustics analysis, particularly the energy decay analysis. So far there are no quantitative rules in the published room-acoustic literature. This Section discusses the sufficient resolution for building the energy-time function $h^2(t_k)$, that is also decisive for the corresponding resolution of Schroeder decay functions.

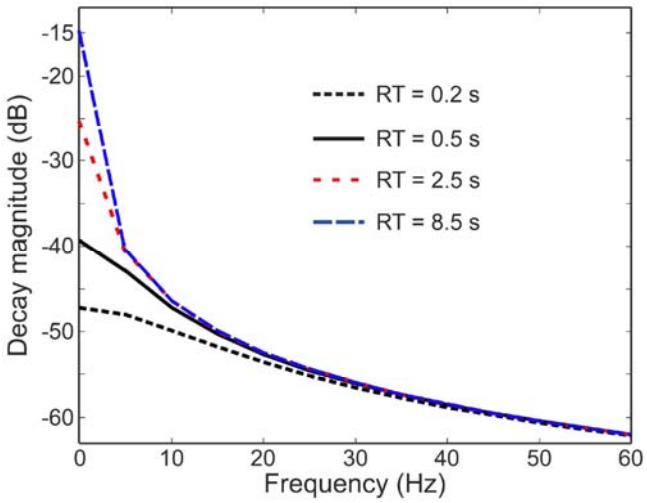

Figure 3. Magnitude spectra of exponential decay functions for different reverberation time quantity of T_1 = 0.2, 0.5, 2.5, and 8.5 s.

This resolution discussion begins with the Schroeder decay model in Eq. (2). In the current state of technology, acousticians can achieve experimental measurements of RIRs with a peak-to-noise ratio on order of >50 dB, often it can reach 70 dB. Furthermore, the noise term $\theta_0(t_k - t_K)$ represents much slower decaying changes in comparison with the exponential decays (see for example, Fig. 2). In addition, in multiple slope characteristics, auditorium acousticians are primarily concerned with ordered profiles,[7] namely $T_1 < T_2 < \cdots < T_S$ and $A_1 > A_2 > \cdots > A_S$ with $A_s = \theta_{(2s-1)}$, that means if multiple decay slopes are ever in the decay data, exponential decays beyond the first rate, specified by T_1, are changing slower in time than the first rate. As for the changing rate concerns, a simplified model

$$H(\mathbf{\Theta}, t_k) \approx \theta_1 \mathrm{e}^{-13.8 t_k / T_1} \tag{3}$$

is sufficient for determining the integration resolution, where the constant terms $\mathrm{e}^{-\theta_{2S} t_K}$, the noise term, and slower exponential decays are ignored when examining the frequency content of the Schroeder decay functions of time. Coefficient θ_1 is the initial value associated with the decay rate of T_1. *Fourier* transform of the decay function in Eq. (3) yields its spectrum in the frequency f domain

$$\underline{H}(f) \approx \frac{\theta_1}{\frac{13.8}{T_1} + \mathrm{j}2\pi f}, \tag{4}$$

with $\mathrm{j} = \sqrt{-1}$. Figure 3 illustrates the magnitude spectra of Eq. (4) for different reverberation time values of T_1 at a fixed value of θ_1 = 0.3. Its magnitude ratio with respect to that at f = 0 can approximately be deduced to

$$\frac{|\underline{H}(f=0)|}{|\underline{H}(f)|} \approx \frac{2\pi f\, T_1}{13.8} \approx \frac{f\, T_1}{2} > 20, \tag{5}$$

with a factor 20 being considered as 10 times of a 'half-power' point along the magnitude spectra. Equation (5) leads to an upper limit frequency f_{u} for the major frequency content of the exponential decay functions to be included. Application of *Nyquist* 's sampling theorem leads to a sampling rate f_{d}, and a time resolution t_Δ for Schroeder decay functions

$$f_{\mathrm{d}} \geq 2.5\, f_{\mathrm{u}} > \frac{100}{T_1} > 20, \text{ and } t_{\Delta} = \frac{1}{f_{\mathrm{d}}}. \quad (6)$$

The above derivations guide acousticians with conditions for determining a sufficient temporal resolution of the resulting energy-time function and Schroeder decay function. Figure 4 (a)-(c) show ETCs derived from the same RIR experimentally measured at a sampling rate of f_{s} = 48 kHz in a well-known concert hall. A square operation is applied for building $h^2(t_k)$ upon block-wise averaging, resulting in three different time resolution/sampling frequency f_{d} = 1000, 500, and 200 Hz, corresponding to a time resolution $t_k - t_{k-1} = t_{\Delta}$ = 1, 2, and 5 ms. Figure 4 (d) compares three resulting Schroeder decay curves, indicating that the resulting sampling frequency f_{d} for the Schroeder decay functions is sufficiently high. In this specific example, reverberation time, T_1 = 2.65 s is estimated, even a f_{d} = 200 Hz represents an oversampling, since it richly fulfills the condition in Eq. (6). The ETCs in Fig. 4 (a) and (b) are redundantly over-sampled. The resulting Schroeder decay curves in Fig. 4 (d) present no significant differences between them.

The sampling rate f_{d} based on Eq. (6) is used to guide an efficient analysis of decay analysis with sufficiently accurate parameter estimates. Therefore, a somewhat oversampling is often set for ETCs / Schroeder decay functions. A moderate oversampling would remove stringent requirement of accurately estimating the reverberation time (the first decay time) in determining the upper limit frequency f_{u} in Eq. (6). Also, the moderate oversampling makes the frequency content of exponential decays more included as Fig. 3 shows, that will make frequency aliasing even more insignificant. With this oversampling, many experimentally measured Schroeder decay functions can be well presented by K data points on order of hundreds, that leads to high efficiency of the data analysis.

4. EFFICIENCY OF ADVANCED ANALYSIS METHODS

Since mid-1990's, several advanced analysis methods have emerged including nonlinear regressions,[4] Bayesian decay analysis.[5] As a number of handful data points can well present the data, as discussed in previous Section, computational load should not be a big concern. For example, the nonlinear regression method [4] runs a small fraction of seconds on current personal computers. For this reason, there should not be big concerns on computational expense, rather it rapidly converges based only on single-slope (S = 1) decay model, which is more suitable for reverberation time estimation. Using a double-slope decay model, the regression convergence requires accurately estimated initial parameter values.

When dealing with multiple-slope decays, Bayesian analysis would be more suitable. Particularly, acousticians are challenged by a higher-level question as how many decay slopes there are in the data before respective decay parameters are reliably estimated. Thanks to Bayesian inference thoroughly reported in the context of room-acoustics decay analysis, the Bayesian framework is well suited to solve two levels of inference, namely the model order selection before any model parameters is to be estimated.[7,8] Bayesian solutions often require random sampling to accomplish the two levels of inferential estimations. Potential users often concern themselves with seemingly sophisticated computational effort. Upon discussions in previous Section, a straightforward estimation of necessary resolution of Schroeder decay function often leads to handful data points to sufficiently present the data. Therefore, the computational expense can be kept as easily manageable in practical implementation, oftentimes they can be implemented with computational load on order of seconds on the current personal computers. With time, such a concern will disappear.

More recently an alternative approach based on artificial neural networks (ANN) [6] has been reported. To train the ANN, Götz *et al.* apply the decay model in Eq. (2), with a preset of potential numbers of slopes, such as 1 to 3, in generating large number (20,000) of predicted Schroeder decay functions by randomly assigning the decay parameters $\boldsymbol{\Theta}$. They try to cover as many decay scenarios as possible and encode all possible predicated decay functions into neurons (weights) in different layers of the ANN during the training phase. After the substantial training effort, the energy decay analysis

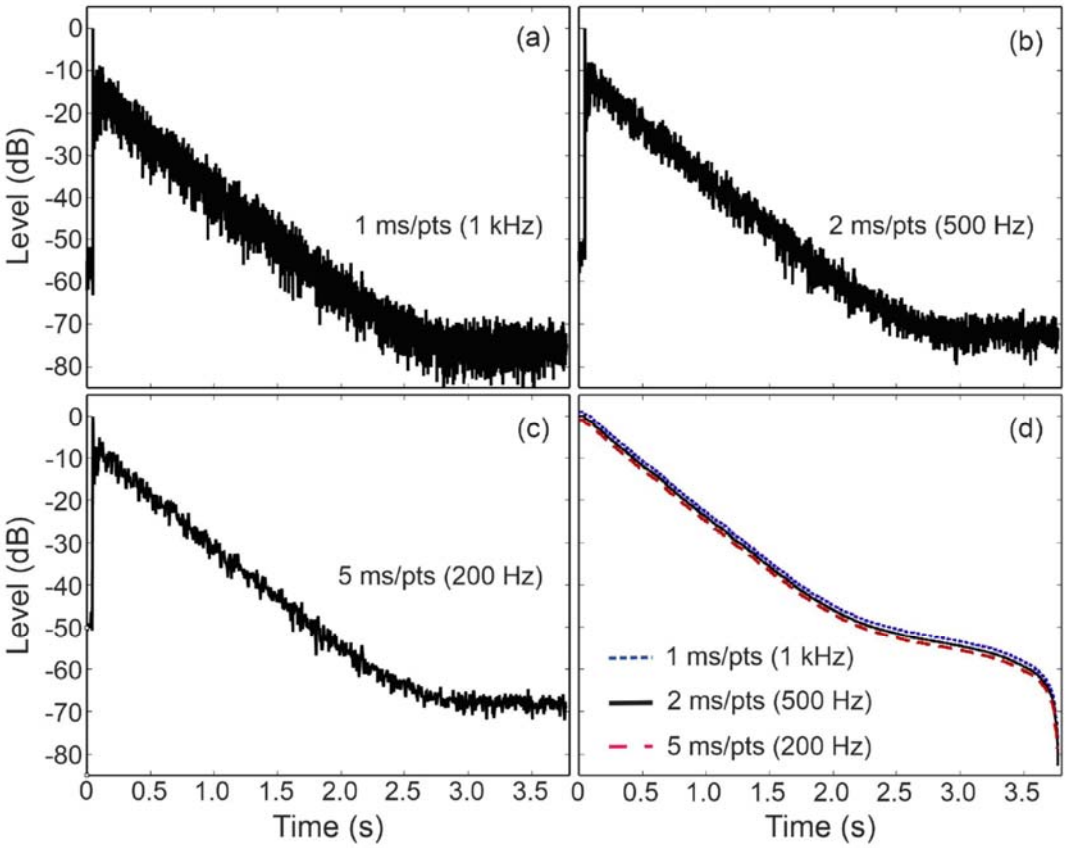

Figure 4. Different resolutions of energy-time curves (ETCs) and corresponding Schroeder decay curves from one experimentally measured room impulse response in a concert hall. (a) ETC at a time resolution of 1 ms/point (equivalent to f_{d} = 1~kHz). (b) ETC at a time resolution of 2 ms/point (f_{d} = 500~Hz). (c) ETC at a time resolution of 5 ms/point (f_{d} = 200~Hz). (d) Three Schroeder decay curves derived from ETCs in (a-c). The curves are slightly shifted for the sake of visualization.

of potentially single or multiple decay characteristics can also be accomplished efficiently. Its efficiency is on a similar order as Bayesian model-based analysis as reported by Götz *et al.*,[6] because the ANN used for their work takes only up to 100 data points. As discussed in the previous Section, one must adjust the temporal resolution of Schroeder integration in order to result in the required small set of the data points.

If the condition is fulfilled, the analysis will not suffer from unacceptable uncertainties. Note that the condition is set for richly retaining the major frequency content of exponential decays. One may adjust the constant factor of Eq. (6) more tightly in obtaining the analysis efficiency at cost of somewhat higher inaccuracies.

5. DECAY PARAMETERS

The advanced methods [5,6] effectively provide decay parameters encapsulated in the Schroeder decay model [Eq. (2)], that serve the decomposition of Schroeder decay functions into individual decay components specified by $A_s(= \theta_{(2s-1)})$, $T_s(= 13.8\,/\theta_{(2s)})$ of exponential decays, particularly for double- or multiple decay slopes. Note that ISO 3382 standard[9] suggests taking the decay functions from -5 dB downwards, to avoid uncertainties at the decay start. In that way, the advanced analysis methods provide the decomposition parameters A_s, T_s used to draw decomposed decay lines [10] as

$$L_s = a_s + b_s\, t_k, \text{ for } 1 \le s \le S\,. \tag{7}$$

with $a_s = 10\lg(A_s)$, $b_s = -10(13.8/T_s)\lg(\mathrm{e})$. Xiang *et al.*[10] also define level differences $L_{\Delta s}$, and turning points for double- or multiple-slope decays. Coefficients a_s, b_s and $L_{\Delta s}$ unambiguously reconstruct the decomposed decay lines in the energy level scales, while the turning points directly indicate at what level and temporal point the previous decay slope transits into the next slower decay slope. Due to the straight-line nature from the model-based decomposition within the logarithmic scale, these parameters can be straightforwardly used to extrapolate decay slope lines to the time point associated with -0 dB using the decomposed straight line models in Eq. (7) when experimenters in practice wish to get the decay parameters associated with other than the time start at -5 dB rather at -0 dB, including the initial decay level values of a_s. From these extended level values, for instance, the level difference from the second decay slope to the starting level (0 dB) is straightforward. As this left the experimenters to convert, there is no need to state the straightforward extrapolation in the published literature.[5,6,10]

6. CONCLUDING REMARKS

This paper discusses energy decay analysis, which is fundamental in auditorium acoustics. The analysis is based on Schroeder integration. To accurately determine energy decay characteristics, a parametric decay model plays a central role. For high efficiency of decay analysis, it is also important to set up conditions for a sufficient time resolution when presenting Schroeder decay functions in digital domain. This condition serves as guidance for acoustic experimenters / analyzers to keep the decay data set presented by as less data points as necessary. In that way, the analysis task using advanced methods, including Bayesian inferential approach and an artificial neural network approach can be accomplished at a high efficiency. This paper clarifies the efficiency issue and other unreasonable expectations/ interpretations encountered in room-acoustics practice, including a straightforward extrapolation of decomposed decay lines.

REFERENCES

1. N. Edwards, J. A. Kemp, and Z. Sü Gül, “Measurement, modelling and subjective responses to the sound decay from coupled volumes in the McPherson room, St Andrews university,” in *Proc. Intl. Con. Acoust.*, ICA2022, Gyeongju, Korea (2022).
2. Z. Sü Gül, E. Odabas, N. Xiang, and M. Caliskan, “Diffusion equation modeling for sound energy flow analysis in multi domain structures,” *J. Acoust. Soc. Am.*, Vol. **145**, 2703–2717, (2019).
3. M. R. Schroeder, “New method of measuring reverberation time,” *J. Acoust. Soc. Am.*, Vol. **37**, 409–412 (1965).
4. N. Xiang, “Evaluation of reverberation times using a nonlinear regression approach,” *J. Acoust. Soc. Am.*, Vol. **98**, 2112–2121 (1995).
5. N. Xiang, P. Goggans, T. Jasa, and P. Robinson, “Bayesian characterization of multiple-slope sound energy decays in coupled-volume systems,” *J. Acoust. Soc. Am.*, Vol. **129**, 741–752 (2011).
6. G. Götz, R. F. Perez, S. J. Schlecht, and V. Pulkki, “Neural network for multi-exponential sound energy decay analysis,” *J. Acoust. Soc. Am.*, Vol. **152**(2), 942-953 (2022).
7. N. Xiang and P. M. Goggans, “Evaluation of decay times in coupled spaces: Bayesian decay model selection,” *J. Acoust. Soc. Am.*, Vol. **113**(5), 2685–2697 (2003).
8. N. Xiang and P. M. Goggans, “Evaluation of decay times in coupled spaces: Bayesian parameter estimation,” *J. Acoust. Soc. Am.*, Vol. **110**(3), 1415–1424 (2001).
9. ISO 3382-1:2009, “Acoustics Measurement of room acoustic parameters, Part 1: Performance spaces,” tech. rep., International Organization for Standardization, Geneva (2009).
10. N. Xiang, Y. Jing, and A. Bockman, “Investigation of acoustically coupled enclosures using a diffusion equation model,” *J. Acoust. Soc. Am.*, Vol. **126**, 1187–1198 (2009).